Interchain Disulfide Bonding in Human IgG2 Antibodies Probed by Site-Directed Mutagenesis

Martin J. Allen,*,† Amy Guo,‖ Theresa Martinez,‖ Mei Han,‖ Gregory C. Flynn,‖ Jette Wypych,‖ Yaoqing Diana Liu,‖ Wenyan D. Shen,§ Thomas M. Dillon,# Christopher Vezina,⊥ and Alain Balland‖

Process and Product Development, Amgen, Inc., Seattle, Washington 98119

Received December 3, 2008; Revised Manuscript Received February 28, 2009

ABSTRACT: Human IgG2 exists as a mixture of disulfide-linked structural isoforms that can show different activities. To probe the contribution of specific cysteine residues to the formation of structural isoforms, we characterized a series of Cys→Ser mutant IgG2 recombinant monoclonal antibodies, focused on the first C_H1 cysteine and the first two hinge cysteines. These residues participate in the formation of structural isoforms that have been noted by nonreduced capillary sodium dodecyl sulfate polyacrylamide gel electrophoresis, reversed-phase high-performance liquid chromatography, and cation exchange chromatography. We show that single Cys→Ser mutants can greatly reduce heterogeneous disulfide bonding in human IgG2 and maintain in vitro activity. The data demonstrate the feasibility of applying site-directed mutagenesis to reduce disulfide bond heterogeneity in human IgG2 while preserving the activity of this therapeutically important class of human antibodies.

Monoclonal antibodies (MAbs)[1] are an increasingly important class of therapeutic proteins. Therapeutic MAbs may be chimeric molecules consisting of murine variable domains and human constant domains, or they may be humanized by replacing much of the murine variable domain with human sequence. More recently, Xenomouse and phage display technologies have made possible the identification of fully human MAbs for therapeutic purposes.

While much attention has focused on proper selection of variable domains, it is also important to consider the heavy chain (HC) isotype in the selection and construction of therapeutic MAb candidates (*1*). The majority of approved therapeutic MAbs are of the IgG class and, of those, most have IgG1 HCs. The IgG1 isotype is a logical choice for programs where effector functions such as antibody-dependent cellular cytotoxicity (ADCC) and complement-dependent cytotoxicity are desired as part of the therapeutic application. When effector functions are not desired other isotypes, including human IgG2 and IgG4, may be considered; there are now examples of human IgG2 and IgG4 MAbs that have been approved for therapeutic use (*1*).

The IgG1, IgG2, and IgG4 isotypes share greater than 90% amino acid sequence identity in their constant domains, but their sequences diverge in the hinge region. The IgG subclasses also differ in their interchain disulfide-bonding patterns (*2*). In IgG1, the HC−light chain (LC) disulfide bond is formed using a Cys residue near the N-terminus of the HC hinge region, whereas in IgG4 this disulfide bond is formed using a Cys residue near the N-terminus of the C_H1 domain. The HC−HC interchain disulfide-bonding patterns are also different between these isotypes; IgG1 shows two parallel hinge-region disulfide bonds linking neighboring HCs, whereas IgG4 shows a mixture of inter- and intra-HC disulfide bonds linking the two hinge-region Cys residues (*3*−*5*). This feature allows IgG4 MAbs to exchange half-molecules and become functionally monovalent and bispecific (*3, 6, 7*). While this may have beneficial consequences in vivo, it also must be considered when selecting the isotype of a therapeutic MAb (*7, 8*).

The disulfide structure of human IgG2 differs from IgG1 and IgG4. Milstein and Frangione demonstrated that in IgG2 the HC−LC disulfide bond is formed between a Cys residue near the N-terminus of C_H1 and the C-terminal Cys residue of the LC (*9*) in a manner similar to that used by IgG4. However, in IgG2 there are four hinge-region disulfide bonds that covalently link adjacent HCs in a ladder-like fashion. Human IgG2 has been reported to form covalent dimers, and it was proposed that one or more of the hinge Cys residues played a role in dimer formation (*10*).

We recently reported the formation of structural isoforms in human IgG2 (*11, 12*). These isoforms were detected by nonreduced capillary sodium dodecyl sulfate polyacrylamide gel electrophoresis (nrCE-SDS) (*13*), reversed-phase high-

* To whom correspondence should be addressed: Current address, Wyeth, 1 Burtt Rd., Andover, MA 01810. Telephone: 978-247-2864. Fax: 978-247-2603. E-mail: mart.j.allen@gmail.com.

† Cell Science and Technology.

‖ Analytical and Formulation Sciences.

§ Protein Science.

Formulation and Analytical Resources.

⊥ Inflammation.

[1] Abbreviations: MAb, monoclonal antibody; HC, heavy chain; LC, light chain; ADCC, antibody-dependent cellular cytotoxicity; SDS-PAGE, sodium dodecyl sulfate polyacrylamide gel electrophoresis; nrCE-SDS, nonreduced capillary sodium dodecyl sulfate polyacrylamide gel electrophoresis; RP-HPLC, reversed-phase high-performance liquid chromatography; MS, mass spectrometry; CEX, cation exchange chromatography; SEC, size exclusion chromatography, NEM, *N*-ethylmaleimide; TFA, trifluoroacetic acid; DTT, dithiothreitol; CNBr, cyanogen bromide, ESI-TOF, electrospray ionization time-of-flight; ELISA, enzyme-linked immunosorbent assay; IC_{50}, 50% inhibitory concentration; CHO, Chinese hamster ovary; GuHCl, guanidine hydrochloride.

10.1021/bi8022174 CCC: $40.75
Published on Web 03/02/2009

Table 1: IgG2 Hinge-Region Cysteine Residue Numbering and IgG2 Mutants Characterized[a]

Glu-Arg-Lys-$\overset{232}{\text{Cys}}$-$\overset{233}{\text{Cys}}$-Val-Glu-$\overset{239}{\text{Cys}}$-Pro-Pro-$\overset{242}{\text{Cys}}$-Pro-Ala

recombinant human IgG2 MAb	mutants characterized
MAb #1	C127S
	C232S
	C233S
	C239S
	C127/232S
	C127/233S
	C232/233S
	C127/232/233S
MAb #2	C127S
	C232S
MAb #3	C127S

[a] Cys127 is located near the N-terminus of the C_H1 domain.

performance liquid chromatography (RP-HPLC) (*14*), and cation exchange chromatography (CEX) (*15*) and were attributed to disulfide scrambling involving the two Cys residues near the N-terminus of the hinge as well as the Cys residue near the N-terminus of the C_H1 domain. Analytical characterization of recombinant human IgG2 has revealed a mixture of disulfide-bonding patterns involving these HC Cys residues and the C-terminal Cys residue of the LC (*12*). At least three distinct structural isoforms have been identified and termed IgG2-A, IgG2-B, and IgG2-A/B. We reported the presence of specific [(HC)-(hinge)-(LC)] covalent complexes by peptide mapping (*12*) and assigned the precise cysteine connectivity of each structural form by partial reduction−alkylation techniques (*16*). In IgG2-A, the LC is covalently linked to the HC via a LC Cys214−HC Cys127 (Kabat numbering (*17*)) disulfide bond, and the four hinge Cys residues form inter-HC disulfide bonds in a parallel fashion as originally described several decades ago (*12*). In IgG2-B, LC Cys214 disulfide bonds to the HC via the hinge-region Cys residue Cys233, whereas HC Cys127 is disulfide linked to hinge residue Cys232 (*16*). IgG2-A/B can be viewed as a hybrid isoform where LC Cys214 disulfide bonds to HC Cys127 in one Fab arm (as in IgG2-A) and to the hinge region in the other Fab arm (as in IgG2-B (*12*)). Analysis of IgG2 affinity purified from the serum of patients treated with human IgG2 drug supports the idea that IgG2-A slowly converts to IgG2-B in vivo through an IgG2-A/B intermediate (*18*). Additionally, we described the precise connectivity of asymmetrical complexes in the IgG2-A/B form, identifying either intrachain (IgG2-A/B_1) or interchain (IgG2-A/B_2) types of complexes (*16*).

To probe the contribution of individual Cys residues to the development of structural isoforms, we prepared a series of Cys→Ser mutants in three different recombinant human IgG2 MAbs, all of which utilized the κ LC (Table 1). These mutants were characterized by nrCE-SDS, RP-HPLC, and peptide mapping. The activity of selected mutants was also examined. Single Cys→Ser replacements greatly reduce the disulfide heterogeneity of human IgG2 while maintaining the activity of the MAbs examined in this study.

MATERIALS AND METHODS

Site-Directed Mutagenesis. Three different IgG2 MAbs were subjected to Cys→Ser mutagenesis. Site-directed mutagenesis was performed by overlapping extension polymerase chain reaction or by using the QuikChange XL site-directed mutagenesis kit (Stratagene, La Jolla, CA). The presence of the mutations encoding the desired amino acid substitutions was confirmed by DNA sequencing.

SDS-PAGE Analysis. SDS-PAGE was performed by using 4−20% Tris-glycine gels according to the method of Laemmli et al. (*19*). Prior to denaturation, the samples were treated with 15 mM iodoacetamide. Samples were denatured at 75 °C for 10 min, and 5 μg of each sample was loaded per lane.

nrCE-SDS Analysis. The analyses were performed on a HP^{3D} CE system (Agilent Technologies, Palo Alto, CA) equipped with a diode array detector. Separations were performed using a bare-fused silica capillary with a total length of 33.0 cm, effective length of 24.5 cm to the detector, an inner diameter (I.D.) of 50 μm, and outer diameter (O.D.) of 365 μm (Agilent Technologies). Antibody separation was monitored at a wavelength of 220 nm. The capillary was preconditioned by rinsing with 0.1 N NaOH at 6 bar for 2 min followed by 0.1 N HCl at 6 bar for 1.5 min. The capillary was filled with Bio-Rad CE-SDS run buffer (Bio-Rad Laboratories, Hercules, CA) at 2 bar for 9 min and then dipped in water to avoid gel carryover. Samples were injected at −10 kV for 20 s and separated at 20 °C under −15 kV for 30 min with 2 bar pressure applied to both capillary inlet and capillary outlet during the separation. The corrected peak area is defined as: corrected peak area $= L_dA/t$, where L_d is the effective length from capillary inlet to the detector, A is the peak area, and t is the migration time.

RP-HPLC analysis. Separation of the IgG2 structural isoforms by RP-HPLC was performed as described previously (*11*).

Tryptic Peptide Mapping of the Nonreduced Molecule. Potential-free cysteine residues present on the monoclonal antibody were alkylated with *N*-ethylmaleimide (NEM). The NEM-labeled material was digested with 10% w/w trypsin in 0.1 M Tris/2 M urea (pH = 8.3) at a concentration of 1 mg/mL for 4 h at 37 °C. The digest reaction was quenched with the addition of 10 μL of 10% trifluoroacetic acid (TFA).

The trypsin-digested sample was analyzed via RP-HPLC with column heating at 60 °C. Mobile phases consisted of (A) 0.12% TFA in water (w/v) and (B) 0.11% TFA in 40:40:20 acetonitrile:isopropanol:water (w/v). Separation was performed on a Jupiter C4 (2.1 × 250 mm) column, conditioned in mobile phase (A) for 20 min. A 100 μg sample of digest was injected, and the peptide fragments eluted at a flow rate of 0.2 mL/min with a gradient of 0−65% (B) in 165 min. Peptide elution was monitored by UV absorbance at 214 nm and online mass acquisition.

Reduction and Alkylation Protocol. The trypsin-digested material was reduced with dithiothreitol (DTT) for 30 min at 55 °C. The antibody was then alkylated with iodoacetic acid (IAA) for 15 min at room temperature. The alkylation reaction was quenched with the addition of DTT.

Mass Spectrometry Conditions for Peptide Mapping. All analyses were performed using a LCQ Deca ion-trap instrument (Thermo-Finnigan, San Jose, CA) equipped with an electrospray source connected to an Agilent 1100 pump (Agilent Technologies). Analysis was carried out in a positive-ion mode using a spray voltage of 5.0 kV, and the MS capillary temperature was maintained at 225 °C. The

instrument was calibrated in the *m*/*z* range of 500−2000 using a mixture of caffeine, MRFA peptide, and Ultramark 1621. Deconvolution of the electrospray ionization mass spectra for the HC and LC was done using ProMass for Xcalibur software. Spectral data for the protein digests were acquired online in the range of 200−2000 *m*/*z*. MS/MS analysis was performed in data-dependent mode. Collision data were obtained using 40% relative collision energy.

Mass Spectrometry Conditions for Reduced Mass Analysis. Mass analysis of the reduced samples was performed by acidic SEC using a polyhydroxyethyl aspartamide column connected in-line to an electrospray ionization time-of-flight (ESI-TOF) mass spectrometer (*20*). Samples were diluted to 2 mg/mL in water. A stock solution of 100 mM TCEP (28.6 mg/ml) in 6.0 M GuHCl was made. The sample was then diluted 1:1 with the reductant/denaturant (TCEP in 6 M GuHCl) and heated to 55 °C for 30 min. The column eluate was directed into an ESI-TOF mass spectrometer (Agilent Technologies) with diverter valve settings selected to direct salt and buffer components to waste. The instrument was tuned and calibrated using Agilent-supplied tuning and calibration solution from 50 to 4000 *m*/*z*. Optimized source and ion transmission system conditions were empirically determined and included a capillary voltage of 5000 V, nitrogen gas rate of 9.0 L/min, and a fragmentor voltage of 415 V. Other settings were typical for this instrument. The mass spectral data for reduced samples were processed using Agilent deconvolution software using default values after selecting appropriate *m*/*z* input and output mass parameters to match the data.

Reduction−Oxidation of Cys→Ser Mutants. Antibody samples at 3 mg/mL were treated with 6 mM cysteine, 0.6 mM cystine, 0.2 M Tris, and 0.9 M GuHCl at pH = 8.0 in 4 °C for 48 h as described previously (*11*). Samples were then buffer exchanged to formulation buffer.

Potency Analysis. Wild-type, Cys127→Ser, and Cys232→Ser MAb #1 potency was evaluated using an ELISA binding assay as previously described (*13*). MAb #1, an antagonist of a cell surface growth factor receptor, was also tested for potency using a cell-based assay that measures receptor activation (*13*). For both assays, the antibodies were tested over a broad range of concentrations, and their activities compared with an internal assay reference standard. MAb #2 was tested for potency as described previously (*11*).

RESULTS AND DISCUSSION

The existence of structural isoforms in MAb #1, MAb #2, and MAb #3 has been recently described (*11*−*13, 16*). These recombinant human IgG2 MAbs utilize identical C_H1, hinge, C_H2, and C_H3 domain sequences, and they also share identical κ C_L domains. The LC and HC variable domains for these MAbs are unrelated as are their antigen-binding specificities. For the present study, we have introduced Cys→Ser mutations into MAb #1, MAb #2, and MAb #3 as detailed in Table 1.

Following the mutagenesis procedure, the DNA fragment containing the desired mutations was cloned into an appropriate expression vector. The Cys127→Ser, Cys232→Ser, Cys233→Ser, Cys232/233→Ser, and Cys239→Ser MAb #1 mutants as well as the Cys127→Ser MAb #3 mutant were stably transfected into a serum-free suspension-adapted Chinese hamster ovary (CHO) cell line (*21*). The Cys127/232→Ser, Cys127/233→Ser, and Cys127/232/233→Ser MAb #1 mutants as well as the Cys127→Ser and Cys232→Ser MAb #2 mutants were transiently transfected into a COS cell expression system previously termed CKE5 (*22*). Wild-type controls for each expression system were also included. The decision to express a given protein in CHO versus COS cells was made based on convenience and does not reflect an inability to express in one host versus another. Following production, the MAbs were purified by protein A affinity chromatography. The Cys127→Ser MAb #3 mutant was further purified, according to methods outlined previously (*23*). Though not extensively optimized, no significant differences in expression or purification yields were seen for any of the mutants relative to their wild-type control (not shown). Incorporation of the mutations was verified on the purified products by SEC-MS of the reduced molecules (*20*). The results listed in Table 2 show that the mass differences anticipated from the changes in amino acid sequence were confirmed for many MAb #1 mutants. In addition, the mass data showed that the major glycan structures were complex-type biantennary fucosylated structures, typical of recombinant antibodies (*16*), indicating that the presence of point mutations had no impact on the *N*-glycosylation pattern.

Table 2: Reduced Mass Analysis of Wild-Type and Cys→Ser MAb #1 Mutants[a]

samples	observed mass (Da)	theoretical mass (Da)	error (ppm)	species assignment
reference standard	50121.86	50122.40	10.77	0 Gal, pE
	50283.84	50284.54	13.92	1Gal, pE
	23357.98	23357.98	0.00	LC
MAb #1 wild-type	50122.01	50122.40	7.78	0Gal, pE
	50284.03	50284.54	10.14	1 Gal, pE
	23357.98	23357.98	0.00	LC
MAb #1 C127S	50105.96	50106.40	8.78	0Gal, pE
	50268.1	50268.54	8.75	1 Gal, pE
	23357.99	23357.98	0.43	LC
MAb #1 C232S	50105.99	50106.40	8.18	0 Gal, pE
	50268.14	50268.54	7.96	1 Gal, pE
	23358.01	23357.98	1.28	LC
MAb #1 C233S	50105.99	50106.40	8.18	0 Gal, pE
	50268.17	50268.54	7.36	1 Gal, pE
	23358.01	23357.98	1.28	LC
MAb #1 C232/233S	50089.86	50090.40	10.78	0 Gal, pE
	50252.06	50252.54	9.55	1 Gal, pE
	23358.04	23357.98	2.57	LC
MAb #1 C239S	50105.64	50106.40	15.17	0 Gal, pE
	50267.77	50268.54	15.32	1 Gal, pE
	23358.00	23357.98	0.86	LC

[a] The reduced reference, wild-type, and mutants were analyzed by SEC-MS. Accuracy of the HC mass measurements corroborates the expected mutations. Gal, galactose, refers to HC glycosylated by a typical biantennary N-linked glycan capped by 0 or 1 galactose; pE, pyroglutamic, resulting from cyclization at N-terminus of the HC.

SDS-PAGE Analysis of Cys→Ser Mutants. SDS-PAGE analysis was performed on MAb #1 mutants listed in Table 1, and the results are shown in Figure 1. Wild-type MAb #1 and the Cys232→Ser mutant show completely assembled HC_2LC_2 antibody under nonreducing conditions, demonstrating complete interchain disulfide bond formation for these MAbs. Under these conditions the Cys127→Ser and Cys239→Ser single mutants and the Cys127/232→Ser and Cys232/233→Ser double mutants also show completely assembled HC_2LC_2 antibody with minor low molecular weight bands, demonstrating the nearly complete formation of fully assembled disulfide-linked antibody for those mutants. More significant low molecular weight species were

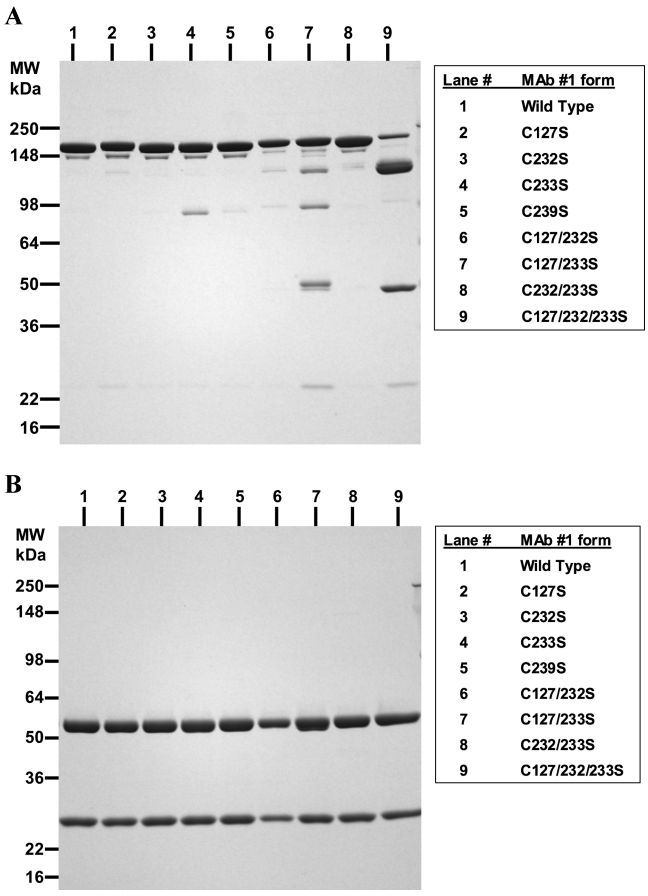

FIGURE 1: SDS-PAGE analysis of wild-type and Cys→Ser MAb #1 mutants. Proteins were analyzed under nonreducing (A) or reducing (B) conditions. Under nonreducing conditions, the minor band migrating just below the main band for all samples, except lane 9, has been previously shown to be a HC−HC−LC covalent form (*13*). Positions of molecular weight markers are indicated.

seen for the Cys233→Ser, Cys127/233→Ser, and Cys127/232/233→Ser mutants, suggesting incomplete formation of HC−HC and/or HC−LC disulfide bonds. Under reducing conditions, the only bands seen were those expected for the reduced HC and LC, demonstrating that the low molecular weight bands seen for some mutants under nonreducing conditions were not contaminations in the protein preparation, but rather the result of incomplete interchain disulfide bond formation.

The Cys127/232/233→Ser mutant, where all of the Cys residues thought to participate in HC−LC disulfide bonding were mutated to Ser, showed little evidence of a HC_2LC_2 complex under nonreducing conditions (Figure 1A). The minor band that migrated near that of the HC_2LC_2 complex could be the result of inefficient disulfide bonding between the LC and one of the remaining HC Cys residues. Alternatively, this could be the result of a complex unique to the mutant, for example HC_3, but the nature of that species was not characterized further. The fact that this and other mutants lacking complete interchain disulfide bonds were purified from our cell cultures demonstrates that the efficient formation of interchain disulfide bonds is not a requisite for IgG2 antibody secretion from mammalian cells.

nrCE-SDS Analysis of Cys→Ser Mutants. As noted previously, human IgG2 but not human IgG1 resolves into two separate forms when analyzed by nrCE-SDS (*12, 13*). Wild-type and mutant MAb #1, MAb #2, and MAb #3 were analyzed by nrCE-SDS, and the results are shown in Figure 2. While wild-type IgG2 MAbs showed two distinct peaks (Figure 2), the single and double mutants involving Cys127 (Figure 2), Cys232 (Figures 2A,B), or Cys233 (Figure 2A) resolved into single HC_2LC_2 complexes. In preliminary experiments, the disulfide bond involving Cys239 was the most sensitive to limited reduction (data not shown). The Cys239→Ser mutant showed evidence of structural isoforms by nrCE-SDS, albeit with ratios different than wild-type (Figure 2A). This may be the result of altered flexibility in the hinge region. When this finding is combined with the peptide mapping results below, we conclude that Cys239 likely does not participate directly in the formation of structural isoforms.

The nrCE-SDS data along with the SDS-PAGE data above demonstrate the plasticity in HC−LC disulfide bonding for human IgG2. Mutation of HC Cys127, the residue historically thought to disulfide bond with the LC, did not significantly affect the efficiency of covalent HC−LC association. Similarly, single mutations of Cys232 or Cys233→Ser also allowed for HC−LC covalent association, although there is evidence of lower molecular weight species for the Cys233→Ser mutant (Figures 1A, 2A). Furthermore, the Cys127/232→Ser and Cys232/233→Ser double mutants also showed formation of the covalent HC_2LC_2 complex (Figures 1A, 2A). While the Cys127/233→Ser mutant did form a covalent complex migrating at the expected molecular weight for HC_2LC_2, several low molecular weight species were also seen, indicating that HC−LC disulfide bonding was less efficient for that mutant (Figures 1A, 2A). This may indicate that the LC shows a preference for disulfide bonding to HC Cys233; Martinez et al. (*16*) have previously noted that in the natural symmetric IgG2-B complex both LCs disulfide bond to the HC at Cys233, whereas in natural asymmetric IgG2-A/B complexes LC disulfide bonded to the HC at Cys232. Taken together, the data both in this report and reported previously demonstrate that in human IgG2 with κ C_L, the LC is capable of disulfide bonding with the HC at either of three positions, Cys127, Cys232, or Cys233.

Yoo et al. (*10*) have previously reported the existence of covalent dimers for human serum IgG2 and for human IgG2 produced using a recombinant expression system. These authors speculated that the covalent dimers could be the result of disulfide bonding between hinge Cys residues in neighboring molecules. In our expression system, we do not see evidence for significant dimer formation. In this study, we saw no evidence for covalent dimers by SDS-PAGE (Figure 1A) or CE-SDS (Figure 2A). Additionally, Van Buren et al. (*24*) have reported less than 3% dimers in human IgG2 even after 15 weeks at 37 °C at pH = 5.0 or 6.0. Therefore, we are unable to confirm that the dimer formation seen by Yoo et al. was through any of the mutated hinge-region Cys residues. It is unclear why we have not seen dimer formation, whereas Yoo et al. (*10*) observed such complexes. For the recombinantly expressed molecules, it is possible that differences in the expression and purification procedures may account for the differences observed in dimer formation. It is also possible that the IgG2 dimers seen in human serum are the result of disulfide bonding between variable domain Cys residues. We have noted higher order complexes unrelated to structural isoforms in recombinant human IgG2 MAbs containing Cys residues in complementarity-determin-

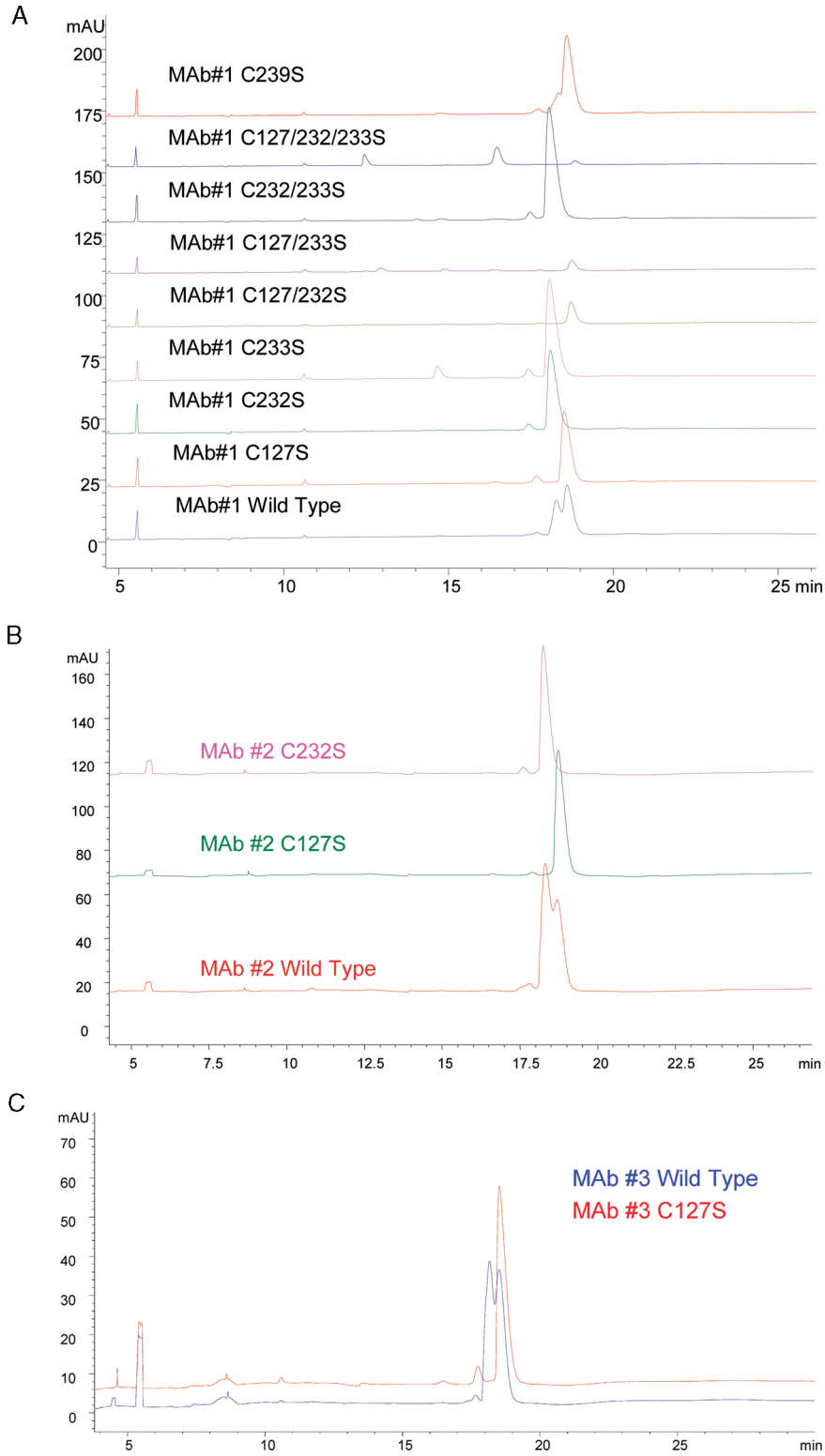

FIGURE 2: nrCE-SDS electropherograms for MAb #1 (A), MAb #2 (B), and MAb #3 (C) wild-type and mutants.

ing regions (unpublished result). It is possible that similar interactions contribute to the higher order structures previously seen for the IgG2 analyzed from human serum.

RP-HPLC Analysis of Cys→Ser Mutants. IgG2 MAbs show multiple peaks when analyzed by nonreduced RP-HPLC, whereas IgG1 typically elutes as a single peak (*11, 12*). The MAb #2 and MAb #3 Cys→Ser mutants were analyzed by nonreduced RP-HPLC, and the results are shown in Figure 3. MAb #1 is not well resolved by RP-HPLC. This is due to multiple levels of heterogeneities between the IgG2s examined in this study, such as glycosylation and partial N-terminal cyclization, unrelated to the concept of structural isoforms, influencing MAb #1 behavior on RP-HPLC. Therefore, MAb #1 mutants were not analyzed by the RP-HPLC technique.

The Cys127→Ser mutation causes the LC to completely disulfide bond to the HC in the hinge region and removes the C_H1−hinge disulfide bond. Therefore, this mutation results in a form not seen in wild-type preparations. For both MAb #2 and MAb #3, the Cys127→Ser mutant was resolved into two peaks that eluted later than the majority of the wild-

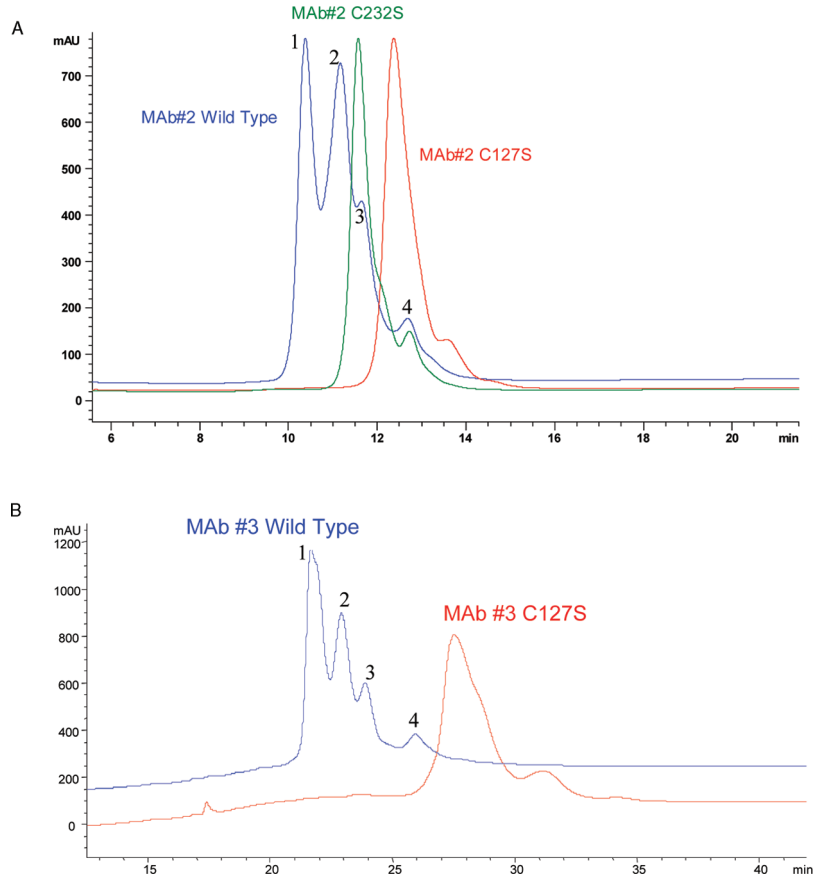

FIGURE 3: RP-HPLC analysis of MAb #2 (A) and MAb #3 (B) mutants. Peak numbering for the wild-type molecule is indicated.

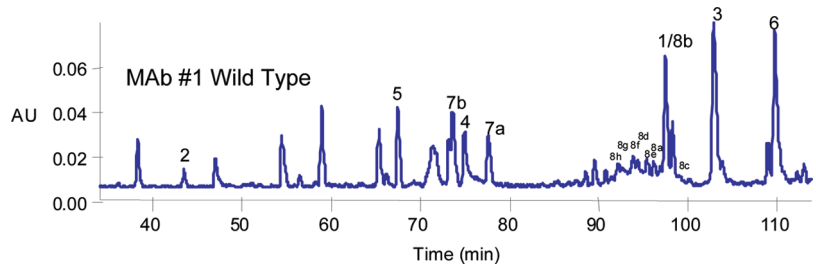

FIGURE 4: Tryptic mapping of nonreduced MAb #1 wild-type (AU, absorbance units).

type IgG2, indicating increased hydrophobic surface area for that mutant (Figure 3). For MAb #2, the major peak elutes at a similar time as peak #4 for the wild-type parent (Figure 3A). Peptide mapping has shown that peak #4 corresponds to an IgG2-A type isoform where the LC is disulfide bonded to the HC at Cys127. Since the Cys127→Ser mutant lacks the ability to form this bond, we conclude that elution time by RP-HPLC does not provide a signature profile for correlating wild-type isoforms with those present in the Cys127→Ser mutant. This is consistent with the RP-HPLC results for the MAb #3 Cys127→Ser mutant that elutes significantly later than any of the wild-type isoforms (Figure 3B).

The MAb #2 Cys232→Ser mutant eluted at a time similar to peak #3 for the wild-type parent (Figure 3A). Given the results above, this may be coincidental or it may reflect the nature of the LC−HC disulfide bond present in this mutant. Peak #3 is known to correspond to an IgG2-A form where the LC disulfide bonds to HC Cys127. The peptide mapping results below demonstrate that this bond is formed in the Cys232→Ser mutants, and, therefore, RP-HPLC may reflect the HC−LC connectivity for that mutant.

Tryptic Peptide Mapping of the Nonreduced Molecule. We previously documented the use of peptide mapping of nonreduced molecules as an effective technique to analyze IgG2 structural isoforms (*12, 16*). Similarly in this study, a tryptic map of the nonreduced molecule was used to identify the disulfide-linked heteropeptides of the wild-type, Cys127→Ser, and Cys232→Ser MAb #1 mutants. To avoid disulfide scrambling, potential free cysteine residues present on the MAb were alkylated with *N*-ethylmaleimide (NEM) in acidic conditions (*25*). The NEM-labeled material was digested with trypsin, and the reaction was quenched with TFA. The resulting fragments were separated by RP-HPLC and analyzed by online mass detection. Disulfide pair assignments were made by identification of bridged peptides using mass analysis (Figure 4, Table 3).

Trypsin cleavage of nonreduced wild-type MAb #1 generated several peptides that contained only one cysteine residue

Table 3: Mass Measurement of Disulfide-Linked Peptides from Wild-Type MAb #1[a]

Disulfide-Linked fragments	Residues	Linkages	Domain	Theoretical Mass(Da)	Experimental Mass(Da)
1	(H)1-43: (H)81-94	(H)Cys22 - (H)Cys92	V_H	6031.7	6031.4
2	(H)117-129: (L)212-214	(H)Cys127 - (L)Cys214	C_H1,C_L	1535.7	1535.8
3	(H)130-145: (H)146-213	(H)Cys142 - (H)Cys208	C_H1	8073.9	8074.1
4	(H)269-305: (H)340-341	(H)Cys274 - (H)Cys340	C_H2	3986.8	3989.6
5	(H)383-393: (H)447-470	(H)Cys390 - (H)Cys456	C_H3	3847.4	3847.5
6	(L)19-42: (L)62-103	(L)Cys23 - (L)Cys88	V_L	7270.0	7270.5
7	(L)127-142: (L)191-207	(L)Cys134 - (L)Cys194	C_L	3558.1	3558.5
8a$(H_{15\text{-}16})_2$	(H)228-261:(H)228-261	(H)Cys232-(H)Cys232	Hinge	5610.9	5610.3
8b $(H_{16})_2$	(H)232-261:(H)232-261	(H)Cys233-(H)Cys233	Hinge	5354.6	5356.7
8c ($H_{15\text{-}16}$:H_{16})	(H)228-261:(H)232-261	(H)Cys239-(H)Cys239 (H)Cys242-(H)Cys242	Hinge	5482.6	5480.9
8d H_{10}:$(H_{16})_2$:L_{18}	(H)228-261 (H)232-261 (H)117-129 (L)212-214		Hinge, C_H1,C_L	6892.3	6889.4
8e H_{10}:$(H_{15\text{-}16})_2$:L_{18}			Hinge, C_H1,C_L	7148.3	7145.9
8f H_{10}:($H_{15\text{-}16}$:$_{16}$):L_{18}			Hinge, C_H1,C_L	7020.3	7016.4
8g $(H_{10})_2$:$(H_{15\text{-}16})_2$:$(L_{18})_2$			Hinge, C_H1,C_L	8682.1	8680.4
8h $(H_{10})_2$:($H_{15\text{-}16}$:$_{16}$):$(L_{18})_2$			Hinge, C_H1,C_L	8554.1	8550.4

[a] The disulfide-linked fragments are tabulated according to the peak labels shown in Figure 4.

and were joined to form seven disulfide-linked fragments (peaks 1−7, Figure 4, Table 3). The identified IgG2 disulfide linkages are as follows (Table 3): HC: Cys22-Cys92, Cys142-Cys208, Cys274-Cys340, and Cys390-Cys456 (Kabat numbering) and LC: Cys23-Cys88, Cys134-Cys194, and interchains HC Cys127-LC Cys214. These disulfide bonds correspond to interchain connectivity and to the intrachain loops: V_H, C_H1, C_H2, C_H3, V_L, and C_L of human IgG2 modeled from the X-ray crystallography structure of IgG1 (*4*). These experimental results provide evidence that the recombinant molecule has the expected human IgG2 disulfide bonds in these regions of the molecule.

Mass measurements for the IgG2 tryptic peptides were examined to further elucidate hinge-region structures. Mass data showed that the hinge region was found, though at low levels, as a dimer of peptide 232−259 (peptide $H_{16,}$ Kabat numbering) with four cysteine bridges in total formed between Cys232, Cys233, Cys239, and Cys242. This structure corresponds to the previously described human IgG2 hinge region (*9*). We denote this molecular form IgG2-A (*11, 12*). When the tryptic digest was reduced and alkylated, however, the fragment H_{16} recovery was as expected. We previously reported that the digest of the nonreduced molecule generated the expected fragment, but only a fraction eluted as a conventional dimer (*12, 16*). The conventional hinge dimer was found to represent only 15−20% of the total hinge content. Analysis by mass spectrometry showed that the additional hinge fractions were separated in a series of peaks between 92 and 100 min and contained tryptic peptide H_{16} (hinge) covalently linked to peptides H_{10} (HC) and L_{18} (LC) (peak 8 a−h, Figure 4, Table 3). Based on the expected structure, however, peptides H_{10} and L_{18} would instead form only the interchain connection C_H1-C_L. As described in our previous reports, the hinge complexes are either symmetrical, connecting two Fabs to the hinge through disulfide bridges, or asymmetrical, connecting one Fab to the hinge (*12*). The symmetrical arrangement, in molecules we denote IgG2-B, corresponds to tryptic peptides of the form [$(H10)_2$-$(H16)_2$-$(L18)_2$] and the asymmetrical arrangement, in IgG2-A/B, to tryptic peptides of the form [(H10)-$(H16)_2$-(L18)] (*16*).

We compared the nonreduced tryptic maps of wild-type, Cys127→Ser, and Cys232→Ser MAb #1 (Figures 4−6, Tables 3−5). The results showed that in all molecules six disulfide-linked peptides, peaks 1 and 3−7, were comparable. Only two disulfide-linked peptides, peak 2 (C_H1-C_L connection) and peak 8 (hinge complexes), had their relative distribution modified according to the type of mutation. Analysis by mass spectrometry of the fractions from the

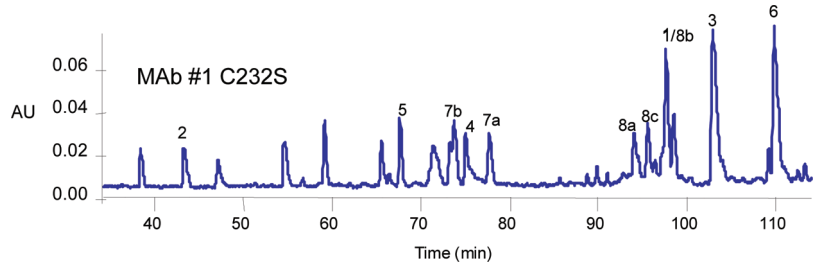

FIGURE 5: Tryptic mapping of the nonreduced C232S MAb #1 mutant.

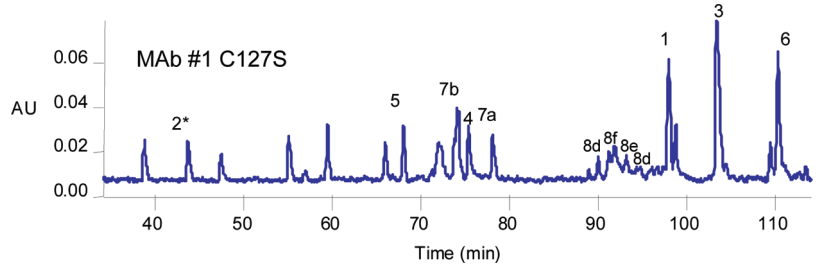

FIGURE 6: Tryptic mapping of the nonreduced C127S MAb #1 mutant.

Table 4: Mass Measurement of Disulfide-Linked Peptides from the Cys232→Ser MAb #1 Mutant[a]

Disulfide-Linked fragments	Residues	Linkages	Domain	Theoretical Mass(Da)	Experimental Mass(Da)
1	(H)1-43: (H)81-94	(H)Cys22 - (H)Cys92	V_H	6031.7	6029.9
2	(H)117-129: (L)212-214	(H)Cys127 - (L)Cys214	C_H1,C_L	1535.7	1535.9
3	(H)130-145: (H)146-213	(H)Cys142 - (H)Cys208	C_H1	8073.9	8076.6
4	(H)269-305: (H)340-341	(H)Cys274 - (H)Cys340	C_H2	3986.8	3989.5
5	(H)383-393: (H)447-470	(H)Cys390 - (H)Cys456	C_H3	3847.4	3847.5
6a	(L)19-42: (L)62-103	(L)Cys23 - (L)Cys88	V_L	7271.0	7270.6
6b	(L)19-45: (L)62-103	(L)Cys23 - (L)Cys88	V_L	7567.2	7566.6
7a	(L)127-142: (L)189-207	(L)Cys134 - (L)Cys194	C_L	3822.9	3823.5
7b	(L)127-142: (L)191-207	(L)Cys134 - (L)Cys194	C_L	3558.1	3558.4
8a $(H_{15\text{-}16})_2$	(H)228-261:(H)228-261	(H)Cys233-(H)Cys233	Hinge	5580.9	5581.4
8b $(H_{16})_2$	(H)232-261:(H)232-261	(H)Cys239-(H)Cys239	Hinge	5324.6	5324.4
8c ($H_{15\text{-}16}$:H_{16})	(H)228-261:(H)232-261	(H)Cys242-(H)Cys242	Hinge	5452.6	5453.1

[a] The disulfide-linked fragments are tabulated according to the peak labels shown in Figure 5.

Cys127→Ser mutant (Figure 6, Table 5) showed tryptic peptide H_{16} (hinge) covalently linked to the peptide L_{18} (LC). This arrangement, with only the LC disulfide linked to the hinge, does not exist in the wild-type molecule. Analyses performed on the disulfide-linked complexes separated from the Cys233→Ser mutant (Supporting Information, Figure S1, Table S1) and Cys232/233→Ser mutant (Supporting Information, Figure S2, Table S2) molecules showed only hinge dimer $(H16)_2$ and $(H15\text{-}16)_2$. This result shows that mutation of cysteine in the upper hinge region eliminates the structural isoforms and generates an IgG2-A-like form.

Analysis by mass spectrometry shows that fractions from the Cys239→Ser mutant were comparable to the wild-type control. This mutant contained tryptic peptide H_{16} (hinge) covalently linked to peptides H_{10} (HC) and L_{18} (LC) in the symmetrical and asymmetrical complexes typical of IgG2 isotype (data not shown). This result indicates that Cys239 in the lower hinge region is not involved in the structural isoforms.

Isolation of Disulfide-Linked Heteropeptides. The disulfide bond structure of the mutants was further characterized by isolation of specific disulfide-linked heteropeptides. We applied our method of combined chemical and enzymatic cleavage with size-exclusion chromatography under denaturing conditions (dSEC) to purify preparative amounts of disulfide-linked peptides, as described previously (*16*). To minimize the possibility of disulfide scrambling, reactive cysteines were blocked by treatment with the alkylating reagent, NEM, at an acidic pH. The next step simplified the analysis by reducing the size of the antibody to a section containing the disulfide-linked fragments. Treatment of MAb #1 with cyanogen bromide (CNBr) cleaved the LC at a single

Table 5: Mass Measurement of Disulfide-Linked Peptides from Cys127→Ser MAb #1 Mutant[a]

Disulfide-Linked fragments	Residues	Linkages	Domain	Theoretical Mass(Da)	Experimental Mass(Da)
1	(H)1-43: (H)81-94	(H)Cys22 - (H)Cys92	V_H	6031.7	6031.4
2(S) not linked	(H)124-135	(H)Ser127	C_H1	1213.7	1214.6
3	(H)136-149: (H)150-212	(H)Cys146 - (H)Cys202	C_H1	8073.9	8074.1
4	(H)130-145: (H)146-213	(H)Cys142 - (H)Cys208	C_H2	3986.8	3989.6
5	(H)269-305: (H)340-341	(H)Cys274 - (H)Cys340	C_H3	3847.4	3847.5
6	(H)383-393: (H)447-470	(H)Cys390 - (H)Cys456	V_L	7270.0	7270.5
7	(L)19-42: (L)62-103	(L)Cys23 - (L)Cys88	C_L	3558.1	3558.5
8a $(H_{15\text{-}16})_2$	(H)228-261:(H)228-261	(H)Cys232-(H)Cys232 (H)Cys233-(H)Cys233 (H)Cys239-(H)Cys239 (H)Cys242-(H)Cys242	Hinge	5610.9	5610.3
8b $(H_{16})_2$	(H)232-261:(H)232-261		Hinge	5354.6	5356.7
8c ($H_{15\text{-}16}$:H_{16})	(H)228-261:(H)232-261		Hinge	5482.6	5480.9
8d L_{18}:$(H_{16})_2$:L_{18}	(H)228-261 (H)232-261 (L)212-214		Hinge, C_L	5964.3	5964.2
8e L_{18}:$(H_{15\text{-}16})_2$:L_{18}			Hinge, C_L	6092.3	6095.8
8f L_{18}:($H_{15\text{-}16}$:$_{16}$):L_{18}			Hinge, C_L	6220.3	6220.1

[a] The disulfide-linked fragments are tabulated according to the peak labels shown in Figure 6.

methionine residue, Met-4, and the heavy chain at Met-108, Met-265, Met-425, Met-459, and Met-459. Cleavage by CNBr and buffer exchange, using a 50 kDa molecular weight cutoff spin filter, reduced the complexity of the analysis by reducing the size of the molecule from 150 kDa to a 75 kDa fragment, containing covalently linked C_L, V_L, C_H1, and hinge. Trypsin digestion further reduced the size of the disulfide-linked peptides. The multiple disulfide-linked fragments resulting from sequential cleavage by CNBr and trypsin are depicted in Supporting Information, Figure S3.

CNBr/tryptic fragments were separated by dSEC using a Phenomenex Biosep column in the presence of GuHCl. The dSEC technique separates six peaks, A−F, which were identified by LC-MS (Supporting Information, Figure S4). The hinge region is represented by tryptic peptide H_{16} (Cys232 to Lys261) and also peptide H15-16 (Lys228 to Lys261) due to partial cleavage of the Arg−Lys bond in the upper hinge. Mass measurement showed that the hinge region was found as a dimer of H_{16} (5352 Da), $H_{15\text{-}16}$ (5608 Da), and $H_{15\text{-}16}$:H_{16} (5480 Da) in the wild-type control. In the single mutants (Cys232→Ser, Cys233→Ser, and Cys239→Ser), the hinge region was found as a dimer of H_{16} (5324 Da), $H_{15\text{-}16}$ (5581 Da), and $H_{15\text{-}16}$:H_{16} (5453 Da). In the double mutants (Cys232/233→Ser), the hinge region was found as a dimer of H_{16} (5295 Da), $H_{15\text{-}16}$ (5551 Da), and $H_{15\text{-}16}$:H_{16} (5423 Da).

The remaining heteropeptides involving the hinge region were found in dSEC fraction B for the control and Cys239→Ser mutant (Supporting Information, Figure S4). RP-HPLC and MS analysis showed that the CNBr/trypsin fragment H_{16} is covalently bound to CNBr/trypsin peptides H10 and L18. As we previously reported (*12*), these two peptides, expected to form the HC−LC interchain connection C_H1-C_L in IgG2-A, are engaged in a complex [(HC)−(hinge)−(LC)] interchain disulfide arrangement in IgG2-B and IgG2-A/B (*12*). This result shows that the complex disulfide-linked peptides are arranged similarly in the wild-type and Cys239→Ser mutant. These data are consistent with the noninvolvement of Cys239 in the structural isoforms.

Treatment of the Cys127→Ser MAb #1 mutant by the CNBr/dSEC technique allowed the purification of the $(H16)_2$-$(L18)_2$ complex, specific to that mutant. The cysteine connection was assessed by a partial reduction/alkylation technique as described previously (*16*). In the Cys127→Ser mutant, the LC cysteine Cys214 was connected to HC Cys233 (Supporting Information, Figure S5). This result is in agreement with the disulfide connectivity we described for IgG2-B (*16*).

Reduction−Oxidation (Redox) of Cys→Ser Mutants. Treatment of wild-type IgG2 with cysteine and cystine in the presence of GuHCl causes an enrichment in IgG2-A (*11*). To determine if this treatment would alter the nrCE-SDS profile for the IgG2 mutants, wild-type, Cys127→Ser, Cys232→Ser, and Cys233→Ser MAb #1 proteins were subjected to redox treatment and analyzed by nrCE-SDS. The results are shown in Figure 7. As expected, the redox treatment caused enrichment in nrCE-SDS peak one (which corresponds to IgG2-A) in wild-type MAb #1. Similar treatment did not alter the nrCE-SDS profile for the mutants, demonstrating that these mutations not only reduce disulfide heterogeneity but also eliminate redox induced isoform conversion.

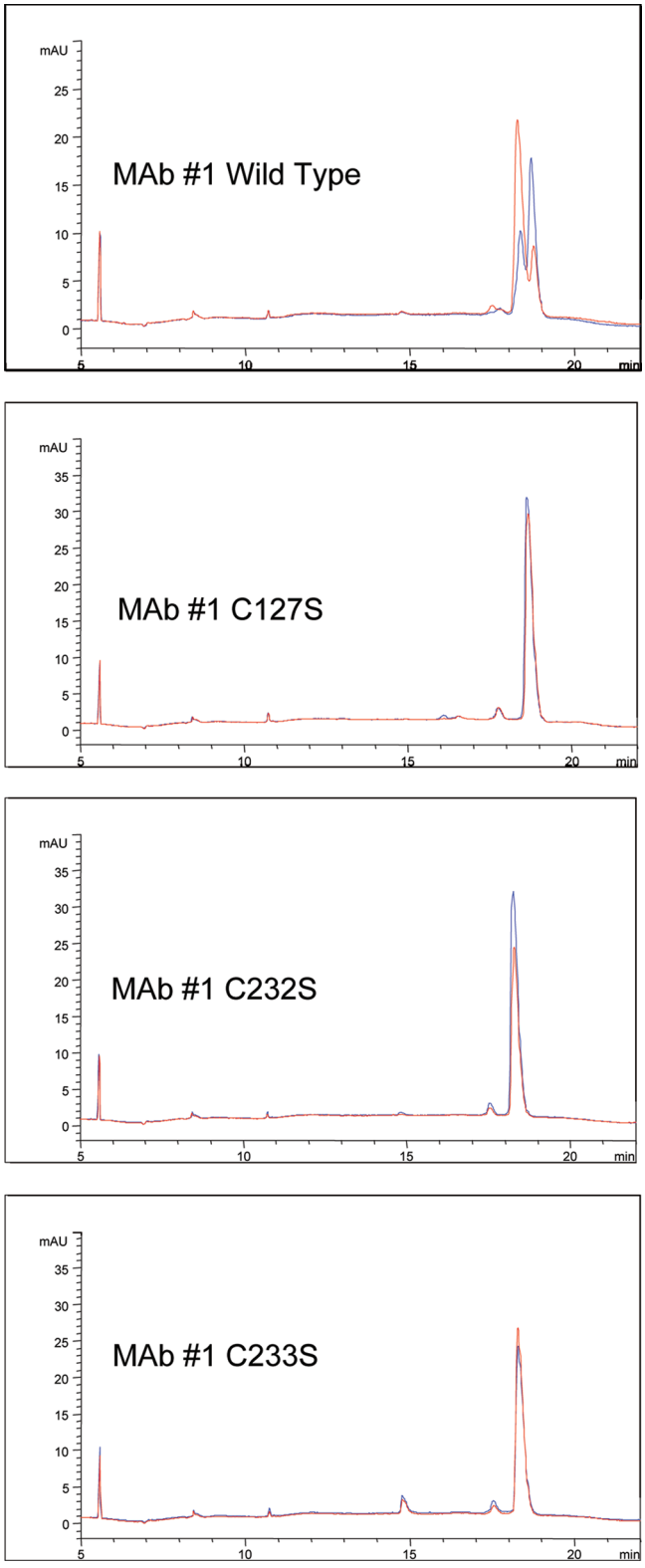

FIGURE 7: nrCE-SDS profiles for redox-treated wild-type, C127S, C232S, and C233S MAb #1. Untreated shown in blue, redox treated shown in red.

Biologic Consequences of Disulfide Rearrangement. To determine if the mutations affected the activity of the human IgG2, wild-type, Cys127→Ser, and Cys232→Ser MAb #1 mutants were analyzed for in vitro activity by two separate assays. Previous work has shown no difference in activity for wild-type MAb #1 enriched in IgG2-B by redox treatment in the absence of GuHCl compared with an untreated control (*13*). For this work, a solid-phase ligand-binding assay and a cell-based assay were employed. The cell-based assay measures the response of the cell by determining receptor phosphorylation. In all cases, the activities of the mutants were indistinguishable from that of the wild-type control (Table 6), demonstrating that for this MAb the mutations do not alter in vitro activity.

Table 6: Potency Values for Wild-Type, Cys127→Ser, and Cys232→Ser MAb #1

	ELISA binding assay	cell-based bioassay
wild-type	108 ± 9[a]	101 ± 9
Cys127→Ser	106 ± 7	91 ± 3
Cys232→Ser	96 ± 3	100 ± 12

[a] Data are the average ± the standard deviation of three determinations normalized against an internal assay standard set to 100.

Unlike MAb #1, preparations of MAb #2 enriched in IgG2-A and IgG2-B forms show 3- to 4-fold differences in activity with IgG2-A, the more active form (*11*). One important hallmark of IgG2-B is the disulfide bonding of the C_H1 region with the hinge. This bond is not present in any of the mutants examined. If this bond is responsible for reducing the activity of IgG2-B, we would expect no reduction in activity for any of the mutants examined. We tested wild-type, Cys127→Ser, and Cys232→Ser MAb #2 for activity in a human chondrocyte cell-based activity detection system as previously described (*11*). The activities of these mutants were comparable to that of the wild-type control (not shown), suggesting that the presence of the C_H1-hinge disulfide bond in IgG2-B is responsible for the reduction in activity for that form of MAb #2.

The in vivo effect of the mutations has not been examined. However, a recent study by Liu et al. (*18*) has demonstrated that for wild-type IgG2, isoform A converts to isoform B in vivo through an isoform A/B intermediate. These authors computed that at equilibrium 71% of IgG2 would be found as IgG2-B, with the remaining as either IgG2-A (7%) or IgG2-A/B (22%). Dillon et al. (*11*) have previously reported that IgG2-A shows higher activity than IgG2-B in about half of the IgG2 directed against cell surface receptors in their test panel. Given that the Cys127→Ser and Cys232→Ser mutations prevent the formation of the C_H1-hinge disulfide bond seen in IgG2-B and, thus, the formation of IgG2-B, it is intriguing to speculate that they could result in more active in vivo preparations of some therapeutic IgG2 MAbs.

The work by Liu et al. (*18*) further demonstrated that the isoforms do not differ in their in vivo clearance rates. Based on those results, we would not expect differential clearance rates for the Cys→Ser mutants described here, although this has not been examined. Alternatively, the presence of the Cys→Ser point mutations could potentially alter their in vivo behavior by mechanisms independent of their effects on isoform composition. For example, IgG2 mutants could stimulate in vivo clearance if the molecules were seen as non-native by the human immune system.

The observed in vivo isoform A to isoform B conversion raises the question of possible disulfide bonding of IgG2 to circulating proteins such as albumin. However, the existing evidence suggests no such disulfide bonding in vivo. For example, Liu et al. (*18*) showed that while the IgG2 isoform ratios change over time after administration, no new protein

species were seen by RP-HPLC for IgG2 that was ligand affinity purified from human serum between 0 h and 13 days post administration. Additionally, if in vivo disulfide bonding to heterologous proteins occurred, it is likely that the glycan profiles of the newly formed covalent complex would differ from that of the original IgG2. A recent study by Chen et al. (*26*) demonstrated nearly identical glycan profiles for IgG2 affinity purified from human serum between 1 h and 13 days post administration. The small changes that were seen over time were attributed to the removal of specific sugars from the IgG2 glycan. Taken together, these observations suggest that clinically administered IgG2 does not disulfide bond to circulating proteins in vivo.

The effect of the mutations on nonantigen binding functions has not been examined. Receptor binding sites required for ADCC activities are known to reside in the lower hinge and C_H2 regions of human IgG1 (*27, 28*). Several mutations in these regions have been shown to modulate Fc receptor binding and ADCC activity of human antibodies (*27, 29*−*31*). Additionally, the absence of a core fucose on the C_H2 *N*-glycan significantly increases the ADCC activity of IgG1 antibodies (*32, 33*) but does not significantly alter the protein structure (*34*). Therefore, subtle changes in the antibody can have dramatic effects on ADCC activity. Dillon et al. (*11*) have previously demonstrated that IgG2-B adopts a more compact structure than IgG2-A and speculated that this may be caused by the presence of the Fab-hinge disulfide bonding. Given the known involvement of the lower hinge and hinge proximal C_H2 region in ADCC, it is possible that there could be differences in Fc receptor binding and ADCC activities for the different isoforms. Shields et al. (*27*) demonstrated that substituting amino acid sequence from the lower hinge region of IgG2 (E233P, L234V, L235A, G236 deleted, EU numbering (*17*)) into IgG1 greatly reduced Fc receptor binding. This IgG2 sequence is retained in the mutants constructed in our work, and, therefore, significant improvements in Fc receptor binding and ADCC may not be anticipated for the IgG2 Cys→Ser mutants. However, given the subtle nature of the mechanisms governing ADCC activity modulation in IgG1, we are unable to conclusively comment on the affects of the mutations on nonantigen binding functions including ADCC.

In conclusion, we have used site-directed mutagenesis and analytical characterization to demonstrate plasticity in the disulfide connectivity of human IgG2 MAbs. It is clear that, for this therapeutically important class of molecules, the LC can disulfide bond to the HC at any of three Cys residues: one in the C_H1 domain (Cys127) and two others in the hinge region (Cys232 and Cys233). Point mutation of these Cys residues greatly reduces the molecular heterogeneity related to disulfide connectivity while preserving in vitro activity.

ACKNOWLEDGMENT

The authors thank David Treiber for the construction of many of the mutants described, Andy Gates and the Research Protein Manufacturing group at Amgen for the production of MAb #1 and MAb #2 proteins, Scott Conrad and Ronald Gillespie for purifying these MAbs, Ling Liu and Rick Jacobsen for cloning and expression of MAb #3 mutants, and Yu Li, Shirley Xue, and Myla Beasley for potency testing. We thank Pranhitha Reddy for helpful discussions and Glenn Begley, Carole Heath, Mike Treuheit, and Dean Pettit for critical reading of the manuscript.

SUPPORTING INFORMATION AVAILABLE

Tables and figures with additional data. This material is available free of charge via the Internet at http://pubs.acs.org.

REFERENCES

1. Salfeld, J. G. (2007) Isotype selection in antibody engineering. *Nat. Biotechnol. 25*, 1369–1372.
2. Frangione, B., Milstein, C., and Pink, J. R. (1969) Structural studies of immunoglobulin G. *Nature 221*, 145–148.
3. Aalberse, R. C., and Schuurman, J. (2002) IgG4 breaking the rules. *Immunology 105*, 9–19.
4. Bloom, J. W., Madanat, M. S., Marriott, D., Wong, T., and Chan, S. Y. (1997) Intrachain disulfide bond in the core hinge region of human IgG4. *Protein Sci. 6*, 407–415.
5. Schuurman, J., Perdok, G. J., Gorter, A. D., and Aalberse, R. C. (2001) The inter-heavy chain disulfide bonds of IgG4 are in equilibrium with intra-chain disulfide bonds. *Mol. Immunol. 38*, 1–8.
6. Schuurman, J., Van Ree, R., Perdok, G. J., Van Doorn, H. R., Tan, K. Y., and Aalberse, R. C. (1999) Normal human immunoglobulin G4 is bispecific: it has two different antigen-combining sites. *Immunology 97*, 693–698.
7. van der Neut Kolfschoten, M., Schuurman, J., Losen, M., Bleeker, W. K., Martinez-Martinez, P., Vermeulen, E., den Bleker, T. H., Wiegman, L., Vink, T., Aarden, L. A., De Baets, M. H., van de Winkel, J. G., Aalberse, R. C., and Parren, P. W. (2007) Anti-inflammatory activity of human IgG4 antibodies by dynamic Fab arm exchange. *Science 317*, 1554–1557.
8. Burton, D. R., and Wilson, I. A. (2007) Immunology. Square-dancing antibodies. *Science 317*, 1507–1508.
9. Milstein, C., and Frangione, B. (1971) Disulphide bridges of the heavy chain of human immunoglobulin G2. *Biochem. J. 121*, 217–225.
10. Yoo, E. M., Wims, L. A., Chan, L. A., and Morrison, S. L. (2003) Human IgG2 can form covalent dimers. *J. Immunol. 170*, 3134–3138.
11. Dillon, T. M., Speed Ricci, M., Vezina, C., Flynn, G. C., Liu, Y. D., Rehder, D. S., Plant, M., Henkle, B., Li, Y., Deechongkit, S., Varnum, B., Wypych, J., Balland, A., and Bondarenko, P. V. (2008) Structural and functional characterization of disulfide isoforms of the human IGG2 subclass. *J. Biol. Chem. 283*, 16206–16215.
12. Wypych, J., Li, M., Guo, A., Zhang, Z., Martinez, T., Allen, M. J., Fodor, S., Kelner, D. N., Flynn, G. C., Liu, Y. D., Bondarenko, P. V., Speed Ricci, M., Dillon, T. M., and Balland, A. (2008) Human IgG2 antibodies display disulfide mediated structural isoforms. *J. Biol. Chem. 283*, 16194–16205.
13. Guo, A., Han, M., Martinez, T., Ketchem, R. R., Novick, S., Jochheim, C., and Balland, A. (2008) Electrophoretic evidence for the presence of structural isoforms specific for the IgG2 isotype. *Electrophoresis 29*, 2550–2556.
14. Dillon, T. M., Bondarenko, P. V., Rehder, D. S., Pipes, G. D., Kleemann, G. R., and Ricci, M. S. (2006) Optimization of a reversed-phase high-performance liquid chromatography/mass spectrometry method for characterizing recombinant antibody heterogeneity and stability. *J. Chromatogr., A 1120*, 112–120.
15. Zhang, Y., Goetze, A., Novick, S., Jocheim, C., Boyce, J. M., Gerhart, M., Qin, X., and Gombotz, W. (2003) Separation and characterization of a monoclonal IgG2 antibody by cation exchange chromatography. *Bioprocessing J. Nov. Dec.* 37–43.
16. Martinez, T., Guo, A., Allen, M. J., Han, M., Pace, D., Jones, J., Gillespie, R., Ketchem, R. R., Zhang, Y., and Balland, A. (2008) Disulfide connectivity of human immunoglobilin G2 structural isoforms. *Biochemistry 47*, 7496–7508.
17. Kabat, E. A., Wu, T. T., Perry, H. M., Gottesman, K. S., and Foeller, C. (1991) In *Sequences of Proteins of Immunological Interest*, 5th ed., Diane Publishing Co., Darby, PA.
18. Liu, Y. D., Chen, X., Zhang-van Enk, J., Plant, M., Dillon, T. M., and Flynn, G. C. (2008) Human IgG2 antibody disulfide rearrangement in vivo. *J. Biol. Chem. 283*, 29266–29272.

19. Laemmli, U. K. (1970) Cleavage of structural proteins during the assembly of the head of bacteriophage T4. *Nature 227*, 680–685.
20. Brady, L. J., Valliere-Douglass, J. F., Martinez, T., and Balland, A. (2008) Molecular mass analysis of antibodies by online SEC-MS. *J. Am. Soc. Mass. Spectrom. 19*, 502–509.
21. Rasmussen, B., Davis, R., Thomas, J., and Reddy, P. (1998) Isolation, characterization and recombinant protein expression in Veggie-CHO: A serum-free CHO host cell line. *Cytotechnology 28*, 31–42.
22. Ettehadieh, E., Wong-Madden, S., Aldrich, T., Lane, K., and Morris, A. E. (2002) Over expression of protein kinase Bα enhances recombinant protein expression in transient systems. *Cytotechnology 38*, 11–14.
23. Shukla, A. A., Hubbard, B., Tressel, T., Guhan, S., and Low, D. (2007) Downstream processing of monoclonal antibodies - Applications of platform approaches. *J. Chromatogr., B 848*, 28–39.
24. Van Buren, N., Rehder, D., Gadgil, H., Matsumura, M., and Jacob, J. (2008) Elucidation of two major aggregation pathways in an IgG2 antibody. *J. Pharm. Sci.* in press.
25. Bures, E. J., Hui, J. O., Young, Y., Chow, D. T., Katta, V., Rohde, M. F., Zeni, L., Rosenfeld, R. D., Stark, K. L., and Haniu, M. (1998) Determination of disulfide structure in agouti-related protein (AGRP) by stepwise reduction and alkylation. *Biochemistry 37*, 12172–12177.
26. Chen, X., Liu, Y. D., and Flynn, G. C. (2009) The effect of Fc glycan forms on human IgG2 antibody clearance in humans. *Glycobiology 19*, 240–249.
27. Shields, R. L., Namenuk, A. K., Hong, K., Meng, Y. G., Rae, J., Briggs, J., Xie, D., Lai, J., Stadlen, A., Li, B., Fox, J. A., and Presta, L. G. (2001) High resolution mapping of the binding site on human IgG1 for Fc gamma RI, Fc gamma RII, Fc gamma RIII, and FcRn and design of IgG1 variants with improved binding to the Fc gamma R. *J. Biol. Chem. 276*, 6591–6604.
28. Sondermann, P., Huber, R., Oosthuizen, V., and Jacob, U. (2000) The 3.2-A crystal structure of the human IgG1 Fc fragment-Fc gammaRIII complex. *Nature 406*, 267–273.
29. Cole, M. S., Anasetti, C., and Tso, J. Y. (1997) Human IgG2 variants of chimeric anti-CD3 are nonmitogenic to T cells. *J. Immunol. 159*, 3613–3621.
30. Lazar, G. A., Dang, W., Karki, S., Vafa, O., Peng, J. S., Hyun, L., Chan, C., Chung, H. S., Eivazi, A., Yoder, S. C., Vielmetter, J., Carmichael, D. F., Hayes, R. J., and Dahiyat, B. I. (2006) Engineered antibody Fc variants with enhanced effector function. *Proc. Natl. Acad. Sci. U. S. A. 103*, 4005–4010.
31. Morgan, A., Jones, N. D., Nesbitt, A. M., Chaplin, L., Bodmer, M. W., and Emtage, J. S. (1995) The N-terminal end of the CH2 domain of chimeric human IgG1 anti-HLA-DR is necessary for C1q, Fc gamma RI and Fc gamma RIII binding. *Immunology 86*, 319–324.
32. Shields, R. L., Lai, J., Keck, R., O'Connell, L. Y., Hong, K., Meng, Y. G., Weikert, S. H., and Presta, L. G. (2002) Lack of fucose on human IgG1 N-linked oligosaccharide improves binding to human Fc gamma RIII and antibody-dependent cellular toxicity. *J. Biol. Chem. 277*, 26733–26740.
33. Shinkawa, T., Nakamura, K., Yamane, N., Shoji-Hosaka, E., Kanda, Y., Sakurada, M., Uchida, K., Anazawa, H., Satoh, M., Yamasaki, M., Hanai, N., and Shitara, K. (2003) The absence of fucose but not the presence of galactose or bisecting *N*-acetylglucosamine of human IgG1 complex-type oligosaccharides shows the critical role of enhancing antibody-dependent cellular cytotoxicity. *J. Biol. Chem. 278*, 3466–3473.
34. Matsumiya, S., Yamaguchi, Y., Saito, J., Nagano, M., Sasakawa, H., Otaki, S., Satoh, M., Shitara, K., and Kato, K. (2007) Structural comparison of fucosylated and nonfucosylated Fc fragments of human immunoglobulin G1. *J. Mol. Biol. 368*, 767–779.

BI8022174